Low-Complexity Estimation of Carrier and Imbalance Parameters in Direct-Conversion Receivers

Wilfried Gappmair, *Member, IEEE*, and Otto Koudelka, *Member, IEEE*

***Abstract*—Due to aggressive goals for future communication systems, direct-conversion receivers are an attractive option in terms of compactness and power dissipation. But the price to pay is an additional impairment introduced by IQ mismatch and DC offset, which might be compensated by appropriately designed DSP algorithms. In this context, recovery of carrier and imbalance parameters has been investigated in many publications available from the open literature. For the current paper, however, we first derive the Cramer-Rao lower bound (CRLB) as the theoretical limit of the jitter variance for joint estimation of carrier frequency/phase, IQ gain/phase imbalance, and DC offset; to this end, the correlation of the noise components – in numerous contributions tacitly neglected – is explicitly taken into account. In the sequel, by means of several simplification steps, we present an approximate closed-form solution for the recovery of carrier and imbalance parameters, whose jitter performance is verified to be close to the CRLB, underlining this way the efficiency of the proposed method.**

***Index Terms*—Parameter estimation, IQ imbalance, DC offset, direct-conversion receiver, computational complexity.**

I. Introduction

DUE to challenging requirements for competitive solutions, direct-conversion transceivers are an attractive option for upcoming communication systems [1], [2], e.g., embodied by a software-defined radio platform [3], [4]. In particular low costs, achieved by small package sizes and reduced power consumption, are an appealing issue in this context. Applying the concept to quadrature mixers, however, this comes at the price of distortions like DC offset and gain/phase imbalance of the involved IQ components. But instead of resorting to expensive heterodyne architectures, which would not show this sort of impairment, intelligent DSP algorithms have been suggested to overcome these imperfections.

Numerous algorithms for compensation of IQ imbalance have been published in the course of time, where it was tried to solve this type of problems not only for receivers, but also for transmitters [5] or even both [6]. A major output of the literature study is that extremely long learning periods are required for adaptive filter structures, if no pilot sequences are employed [7], [8]. Hence, many papers are focused on a pilot-aided (PA) solution, especially when data are transmitted in form of bursts or packets. On the other hand, user data might be exploited by iterative (turbo) methods combining IQ compensation and error correction [9], which provides a performance close to the Cramer-Rao lower bound (CRLB) as the theoretical limit of the jitter variance. Mainly guided by OFDM issues, joint recovery of carrier frequency and IQ imbalance has been investigated in [10]–[12].

For linearly modulated signals and binary pilot sequences, a maximum-likelihood (ML) estimator for joint recovery of carrier phase and IQ phase imbalance has been discussed in [13]. This was followed by an extension of the subject to orthogonal pilots, thus reducing the computational load of the estimation process [14]. Nevertheless, in none of these contributions the correlation of the noise components is taken into account, although this does not hold true in the strict sense for a nonzero IQ phase mismatch [6], [15]. Avoiding this shortcoming and regarding the impact of carrier frequency errors as well, the CRLB has been derived in [16]; since an ML solution for joint recovery of carrier and imbalance parameters turned out to be problematic from both the computational and the stability point of view, the focus was on a low-complex and stable algorithm.

But direct-conversion receivers suffer also from a DC offset caused by self-mixing effects, which has been neglected in [13], [14], and [16]. Motivated by this fact, we will extend the signal model in the current paper so that this sort of imperfection is addressed as well. Again, the key aspect of the estimator framework is on low complexity and stability; on top of that, we compute the CRLB to make sure that our approach is efficient for this extended scenario, too. In contrast to the investigations in [17] and [18], we assume binary pilot sequences and a frequency-flat fading channel to come up with a simplified framework for parameter estimation.

The rest of the paper is organized as follows. In Section II, the signal model for analytical and simulation work is established. Applying the Fisher information matrix, we calculate the CRLB for joint estimation of carrier and IQ mismatch in Section III. Based on the separate extraction of the carrier frequency error and a simplified form of the log-likelihood function, Section IV furnishes a low-complex solution for joint recovery of carrier phase, IQ gain/phase imbalance, and DC offset. Numerical results reflecting the symbol error performance of 4-PSK and 16-QAM signals are presented in Section V. Finally, conclusions are drawn in Section VI.

The paper was presented in part at the IEEE 8^{th} Int. Symposium on Communication Systems, Networks and Digital Signal Processing, Poznan, Poland, July 2012.

W. Gappmair and O. Koudelka are both with the Institute of Communication Networks and Satellite Communications, Graz University of Technology, 8010 Graz, Austria (e-mail: gappmair@tugraz.at).

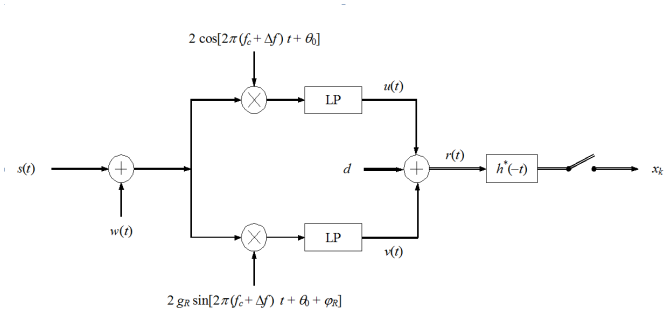

Fig. 1. Basic block diagram of the IQ demodulator architecture.

II. Signal Model

It is assumed that the transmitter is not affected by IQ mismatch and that the independent and identically distributed (i.i.d.) data symbols $c_k = a_k + jb_k$ are zero-mean and normalized to unit variance. In the sequel, these symbols are shaped with the unit-energy baseband pulse $h(t)$. The resulting envelopes $I(t)$ and $Q(t)$ are modulated by the carrier frequency f_c so that the RF signal is given by [19]

$$s(t) = I(t)\cos(2\pi f_c t) + Q(t)\sin(2\pi f_c t), \tag{1}$$

with

$$I(t) = \sum_i a_i h(t - iT)\,, \quad Q(t) = \sum_i b_i h(t - iT), \tag{2}$$

where T denotes the symbol period. At the receiver side, as it is illustrated in Fig. 1, $s(t)$ is corrupted by thermal RF noise $w(t)$; composed of the i.i.d. zero-mean white Gaussian baseband processes $w_I(t)$ and $w_Q(t)$, this is usually expressed as

$$\begin{aligned} w(t) \;=\; & w_I(t)\cos[2\pi(f_c + \Delta f)t + \theta_0] \\ & + w_Q(t)\sin[2\pi(f_c + \Delta f)t + \theta_0]. \end{aligned} \tag{3}$$

For convenient reasons, the carrier frequency offset Δf between transmitter and receiver – typically caused by Doppler shift and oscillator mismatch – forms already part of (3); this holds also true for θ_0, which can be any value between $\pm\pi$, but we simply assume that θ_0 is equal to the carrier phase offset. Furthermore, we assume that the variance of $w_I(t)$ and $w_Q(t)$ is given by $N_0/2$, in our case normalized to the mean signal energy per symbol, i.e., $\sigma_w^2 = 1/(2\gamma_s)$, where $\gamma_s \doteq E_s/N_0$ is defined as the mean signal-to-noise ratio (SNR) per symbol.

Via a mixer stage, impaired by carrier frequency and phase offsets, the received signal is shifted down to the baseband, where higher frequency terms are rejected by a suitably designed low-pass filter (LP). Without loss of generality, it is suggested that both gain and phase imbalances, g_R and φ_R, are just related to the Q-branch [6], which is also reflected by Fig. 1. Consequently, the baseband components are obtained as

$$\begin{aligned} u(t) \;=\; & I(t)\cos(2\pi\Delta f t + \theta_0) \\ & - Q(t)\sin(2\pi\Delta f t + \theta_0) + n_I(t) \end{aligned} \tag{4}$$

and

$$\begin{aligned} v(t) \;=\; & g_R I(t)\sin(2\pi\Delta f t + \theta_0 + \varphi_R) \\ & + g_R Q(t)\cos(2\pi\Delta f t + \theta_0 + \varphi_R) + g_R n_Q(t), \end{aligned} \tag{5}$$

where

$$n_I(t) = w_I(t) \tag{6}$$

and

$$n_Q(t) = w_I(t)\sin\varphi_R + w_Q(t)\cos\varphi_R. \tag{7}$$

Recalling that $w_I(t)$ and $w_Q(t)$ are i.i.d. zero-mean Gaussian processes, each of them with variance σ_w^2, it is clear that $n_I(t)$ and $n_Q(t)$ are also zero-mean Gaussian with variance σ_w^2. But in contrast to $w_I(t)$ and $w_Q(t)$, it is to be pointed out that $n_I(t)$ and $n_Q(t)$ are correlated by the coefficient

$$\rho = \frac{E[n_I(t)n_Q(t)]}{\sqrt{E[n_I^2(t)]E[n_Q^2(t)]}} = \sin\varphi_R. \tag{8}$$

Because of self-mixing effects, the IQ components $u(t)$ and $v(t)$ are affected by a DC offset $d = (d_I,\, d_Q)$, which is also visualized by the signal model in Fig. 1.

In the next step, the baseband signal $r(t)$ passes the matched receiver filter $h^*(-t)$. Assuming a perfectly recovered symbol timing, the corresponding output signal $x(t)$ is sampled appropriately so that we have

$$x_k \doteq r(t) \otimes h^*(-t)|_{t=kT} = d + s_k + n_k, \tag{9}$$

where $\otimes$ denotes convolution, $x_k = (x_{k,I},\, x_{k,Q})$, $s_k = (s_{k,I},\, s_{k,Q})$, and $n_k = (n_{k,I},\, g_R n_{k,Q})$. The noise elements $n_{k,I}$ and $n_{k,Q}$ are zero-mean Gaussian with variance σ_w^2 and correlation coefficient $\rho = \sin\varphi_R$. By introducing the normalized frequency offset $v_0 \doteq \Delta f T$, it is easy to show that the IQ components of the signal samples can be written as

$$\begin{pmatrix} s_{k,I} \\ s_{k,Q} \end{pmatrix} = \underbrace{\begin{pmatrix} \cos(s(k)) & -\sin(s(k)) \\ g_R\sin(z(k)) & g_R\cos(z(k)) \end{pmatrix}}_{X_{\mathbf{\Gamma}(g_R,\varphi_R,\theta_0,v_0)}} \begin{pmatrix} a_k \\ b_k \end{pmatrix}, \tag{10}$$

where $s(k) = 2\pi k v_0 + \theta_0$ and $z(k) = 2\pi k v_0 + \theta_0 + \varphi_R$.

Fig. 2 illustrates the direct-conversion procedure from a different perspective: If we assume that the upper (user) band is shifted by the oscillator frequency $f_c + \Delta f$ down to the baseband, the IQ mismatch of the mixer stage causes an aliasing with the lower (image) band, as it is shown in the sketch. On top of that, we observe that the DC offset emerges as a single spectral line at $f = 0$.

III. Cramer-Rao Lower Bound

Powerful estimates of a parameter vector $\mathbf{u}$ exhibit no bias, i.e., $E[\hat{\mathbf{u}}] = \mathbf{u}$, where $E[\cdot]$ denotes expectation. But powerful estimation is also determined by a jitter (error) variance close to a theoretical limit known as the Cramer-Rao lower bound (CRLB), which is computed via the Fisher information matrix (FIM). For joint estimation of carrier and IQ mismatch, we simply have $\mathbf{u} = (u_1, u_2, u_3, u_4, u_5, u_6) = (g_R, \varphi_R, \theta_0, v_0, d_I, d_Q)$. No nuisance parameters need to be

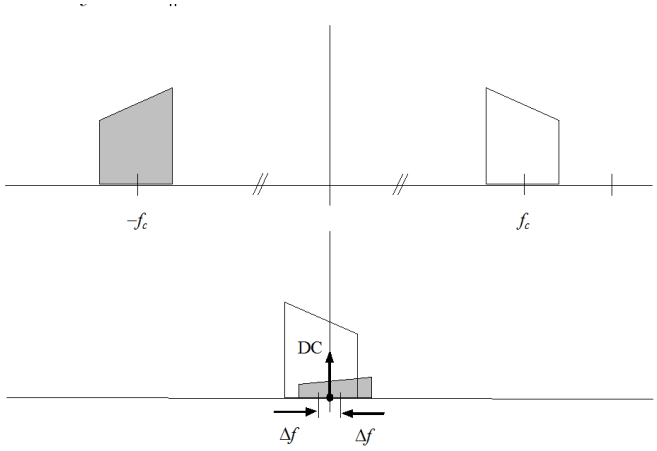

Fig. 2. Power spectrum for a direct-conversion receiver.

considered in this context. Hence, with $\mathbf{x}$ as the received sequence of L independent observables (9), the probability of the deterministic but unknown parameter vector $\mathbf{u}$ is furnished by [20]

$$\begin{aligned}\Pr(\mathbf{x}|\mathbf{u}) &= \prod_{k\in K} \frac{1}{2\pi g_R\sigma_w^2\sqrt{1-\rho^2}} \exp\left(-\frac{\lambda_k}{2g_R^2\sigma_w^2(1-\rho^2)}\right) \\ &= \prod_{k\in K} \frac{1}{2\pi g_R\sigma_w^2\cos\varphi_R} \exp\left(-\frac{\lambda_k}{2g_R^2\sigma_w^2\cos^2\varphi_R}\right),\end{aligned} \tag{11}$$

where $K = \{k_0, k_0+1, \ldots, k_0+L-1\}$ indicates the index range of the observation window and

$$\begin{aligned}\lambda_k &= g_R^2(x_{k,I} - s_{k,I} - d_I)^2 + (x_{k,Q} - s_{k,Q} - d_Q)^2 \\ &-2g_R\sin\varphi_R(x_{k,I} - s_{k,I} - d_I)(x_{k,Q} - s_{k,Q} - d_Q).\end{aligned} \tag{12}$$

The CRLB of the i-th element in $\mathbf{u}$ is provided as [21]

$$\mathrm{CRLB}(u_i) = [\mathbf{I}^{-1}(\mathbf{u})]_{ii} \tag{13}$$

with

$$F_{ij} \doteq [\mathbf{I}(\mathbf{u})]_{ij} = -E_{\mathbf{x}}\left[\frac{\partial^2}{\partial u_i \partial u_j}\log\Pr(\mathbf{x}|\mathbf{u})\right] \tag{14}$$

as the corresponding FIM entry and $E_{\mathbf{x}}[\cdot]$ stands for the expectation with respect to data and noise. Since (11) represents a steadily differentiable function, it is clear that $F_{ij} = F_{ji}$. For binary pilot sequences, the FIM elements are listed in the Appendix.

IV. Low-Complexity Estimator

Based on the log-likelihood function $\Lambda(\mathbf{u}) \doteq \log\Pr(\mathbf{x}|\mathbf{u})$, a maximum-likelihood (ML) algorithm for joint estimation of carrier frequency/phase, IQ gain/phase imbalance, and DC offset can be developed. This is simply achieved by equating the first-order derivatives $\Lambda_i \doteq \partial\Lambda(\mathbf{u})/\partial u_i$ to zero and solving the (nonlinear) set of equations with respect to u_i, $1 \le i \le 6$. Needless to say that there exists no closed-form solution so that we must resort to a numerical procedure, e.g., the Newton-Raphson algorithm [22]. Apart from the computational load, it turned out quickly that this iterative approach suffers from serious stability and convergence problems.

On the other hand, even in the presence of larger IQ imbalance and DC offsets, we learned that frequency errors can be reliably estimated by algorithms well known from the open literature [23], [24], like the method published by Morelli and Mengali (M&M) in [25]. Moreover, as a further simplification step to obtain the remaining parameters, we assume that the correlation of the noise components $n_{k,I}$ and $n_{k,Q}$ is negligible, i.e., $\rho \to 0$, such that the likelihood function (11) reduces to

$$\begin{aligned}\Pr(\mathbf{x}|\mathbf{u}) = \prod_{k\in K} \frac{1}{2\pi\, g_R\sigma_w^2} \exp\Bigg(&-\frac{(x_{k,I} - s_{k,I} - d_I)^2}{2\sigma_w^2} \\ &-\frac{(x_{k,Q} - s_{k,Q} - d_Q)^2}{2g_R^2\sigma_w^2}\Bigg).\end{aligned} \tag{15}$$

Hence, conditioned on the frequency estimate $\hat{v}_0$ achieved by M&M and the simplified likelihood function in (15), we have to manage the parameter vector $\mathbf{u} = (u_1, u_2, u_3, u_4, u_5) = (g_R, \varphi_R, \theta_0, d_I, d_Q)$. After some tedious but straightforward algebra (immaterial constants and factors not depending on u_i are skipped), the related derivatives Λ_i, $1 \le i \le 5$, can be written as

$$\begin{aligned}\Lambda_1 = &-g_R^2\sigma_w^2 + d_Q^2 - 2d_QX_Q + X_{Q2} \\ &+ g_Rd_QX_s\cos(\theta_0+\varphi_R) + g_Rd_QX_c\sin(\theta_0+\varphi_R) \\ &- g_RX_{Qs}\cos(\theta_0+\varphi_R) - g_RX_{Qc}\sin(\theta_0+\varphi_R),\end{aligned} \tag{16}$$

$$\begin{aligned}\Lambda_2 = &\,X_{Qc}\cos(\theta_0+\varphi_R) - X_{Qs}\sin(\theta_0+\varphi_R) \\ &- d_QX_c\cos(\theta_0+\varphi_R) + d_QX_s\sin(\theta_0+\varphi_R) \\ &- \tfrac{1}{2}g_RX_{2s}\cos(2\theta_0+2\varphi_R) - \tfrac{1}{2}g_RX_{2c}\sin(2\theta_0+2\varphi_R),\end{aligned} \tag{17}$$

$$\begin{aligned}\Lambda_3 = &\,\tfrac{1}{2}X_{2s}\cos 2\theta_0 + \tfrac{1}{2}X_{2c}\sin 2\theta_0 \\ &+ d_IX_s\cos\theta_0 + d_IX_c\sin\theta_0 - X_{Is}\cos\theta_0 - X_{Ic}\sin\theta_0,\end{aligned} \tag{18}$$

$$\Lambda_4 = -d_I + X_I - X_c\cos\theta_0 + X_s\sin\theta_0, \tag{19}$$

$$\begin{aligned}\Lambda_5 = -d_Q + X_Q - g_RX_c\sin(\theta_0+\varphi_R) - \\ g_RX_s\cos(\theta_0+\varphi_R),\end{aligned} \tag{20}$$

by using the following definitions:

$$\begin{aligned}X_{Ic} &\doteq \tfrac{1}{L}\sum_{k\in K} a_k\mathrm{Re}[x_k]\cos(2\pi k\hat{v}_0), \\ X_{Is} &\doteq \tfrac{1}{L}\sum_{k\in K} a_k\mathrm{Re}[x_k]\sin(2\pi k\hat{v}_0),\end{aligned} \tag{21}$$

$$\begin{aligned}X_{Qc} &\doteq \tfrac{1}{L}\sum_{k\in K} a_k\mathrm{Im}[x_k]\cos(2\pi k\hat{v}_0), \\ X_{Qs} &\doteq \tfrac{1}{L}\sum_{k\in K} a_k\mathrm{Im}[x_k]\sin(2\pi k\hat{v}_0),\end{aligned} \tag{22}$$

$$\begin{aligned}X_c &\doteq \tfrac{1}{L}\sum_{k\in K} a_k\cos(2\pi k\hat{v}_0), \\ X_s &\doteq \tfrac{1}{L}\sum_{k\in K} a_k\sin(2\pi k\hat{v}_0),\end{aligned} \tag{23}$$

$$\begin{aligned}X_{2c} &\doteq \tfrac{1}{L}\sum_{k\in K} \cos(4\pi k\hat{v}_0), \\ X_{2s} &\doteq \tfrac{1}{L}\sum_{k\in K} \sin(4\pi k\hat{v}_0),\end{aligned} \tag{24}$$

$$X_I \doteq \tfrac{1}{L}\sum_{k\in K}\mathrm{Re}[x_k],\qquad X_Q \doteq \tfrac{1}{L}\sum_{k\in K}\mathrm{Im}[x_k], \tag{25}$$

$$X_{Q2}\doteq\frac{1}{L}\sum_{k\in K}\mathrm{Im}[x_k]^2. \tag{26}$$

Nevertheless, setting the equations (16)–(20) to zero and solving them for $\mathbf{u}=\hat{\mathbf{u}}$, a closed-form solution can not be achieved, although it is to admit that the Newton-Raphson procedure is simpler and much more stable than in the previous case, where frequency offsets and correlation of the noise components had to be considered as well. With $\mathbf{\Lambda}=(\Lambda_1,\Lambda_2,\Lambda_3,\Lambda_4,\Lambda_5)$, the joint estimate is now iteratively computed as

$$\hat{\mathbf{u}}^{(n+1)} = \hat{\mathbf{u}}^{(n)} - \left(\mathbf{J}^{-1}\mathbf{\Lambda}\right)|_{\mathbf{u}=\hat{\mathbf{u}}^{(n)}}, \tag{27}$$

where $J_{ij}\doteq\partial\Lambda_i/\partial u_j$, $1\le i,\,j\le 5$, denotes the (i,j)-th entry of the Jacobian $\mathbf{J}$. Concerning the initialization of the scheme in (27), we figured out that

$$\begin{aligned}&\hat{g}_R^{(0)}=1,\quad \hat{\varphi}_R^{(0)}=0,\\ &\hat{\theta}_0^{(0)}=\arg\left(\sum_{k\in K}c_k^* x_k e^{-j2\pi k\hat{v}_0}\right),\\ &\hat{d}_I^{(0)}=\hat{d}_Q^{(0)}=0,\end{aligned} \tag{28}$$

provides excellent results in terms of stability and convergence. But the computational complexity of (27) is still significant. This is not only due to the involved vector and matrix operations, but also because of the rather intricate expressions forming part of $\mathbf{J}$ and $\mathbf{\Lambda}$. Motivated by this observation, we propose an alternative approach based on an appropriate linearization of (16)–(20), which ends up in a true closed-form solution.

To this end, we will establish a further simplification step in that we ignore the contributions of d_I and d_Q in (16)–(18). This is justified by the fact that the averaging of the FIM entries with respect to a_k causes a block-diagonal structure of the matrix (see Appendix) such that the computation of the DC offset is decoupled from the carrier phase and the IQ gain/phase imbalance. For our estimation problem, this is approximately achieved by sufficiently long pilot sequences with pseudo-random character.

Then, by introducing $\hat{\theta}_0=\hat{\theta}_0^{(0)}+\Delta\theta_0$ as well as assuming that $|\Delta\theta_0|\ll 1$, we immediately obtain the approximations $\cos\hat{\theta}_0 \approx \cos\hat{\theta}_0^{(0)}-\Delta\theta_0\sin\hat{\theta}_0^{(0)}$ and $\sin\hat{\theta}_0\approx\sin\hat{\theta}_0^{(0)}+\Delta\theta_0\cos\hat{\theta}_0^{(0)}$. If we substitute these expressions into (18) by neglecting d_I, the incremental phase offset can be written as

$$\Delta\theta_0=\frac{X_{2s}\cos 2\hat{\theta}_0^{(0)}+X_{2c}\sin 2\hat{\theta}_0^{(0)}-2(X_{Is}\cos\hat{\theta}_0^{(0)}+X_{Ic}\sin\hat{\theta}_0^{(0)})}{2(X_{2s}\sin 2\hat{\theta}_0^{(0)}-X_{2c}\cos 2\hat{\theta}_0^{(0)}+X_{Ic}\cos\hat{\theta}_0^{(0)}-X_{Is}\sin\hat{\theta}_0^{(0)})} \tag{29}$$

Furthermore, with $\hat{g}_R=1+\Delta g_R$ and $|\Delta g_R|\ll 1$, we have that $\hat{g}_R^2\approx 1+2\Delta g_R$, whereas with $\hat{\varphi}_R=\Delta\varphi_R$ and $|\Delta\varphi_R|\ll 1$, we find that $\cos\hat{\varphi}_R\approx 1$ and $\sin\hat{\varphi}_R\approx\Delta\varphi_R$. Inserting this into (16) and (17) by neglecting once more the DC offset, the gain and phase increments are, after some tedious but straightforward algebra, furnished by

$$\Delta g_R=\frac{A_2B_0-A_0B_2}{A_1B_2-A_2B_1},\ \Delta\varphi_R=\frac{A_1B_0-A_0B_1}{A_2B_1-A_1B_2}, \tag{30}$$

where

$$\begin{aligned}A_0&=X_{Q2}-X_{Qc}\sin\hat{\theta}_0-X_{Qs}\cos\hat{\theta}_0-\sigma_w^2,\\ A_1&=-X_{Qc}\sin\hat{\theta}_0-X_{Qs}\cos\hat{\theta}_0-2\sigma_w^2,\\ A_2&=X_{Qs}\sin\hat{\theta}_0-X_{Qc}\cos\hat{\theta}_0,\end{aligned} \tag{31}$$

and

$$\begin{aligned}B_0&=2X_{Qc}\cos\hat{\theta}_0-2X_{Qs}\sin\hat{\theta}_0-X_{2c}\sin 2\hat{\theta}_0-X_{2s}\cos 2\hat{\theta}_0,\\ B_1&=-X_{2c}\sin 2\hat{\theta}_0-X_{2s}\cos 2\hat{\theta}_0,\\ B_2&=2X_{2s}\sin 2\hat{\theta}_0-2X_{2c}\cos 2\hat{\theta}_0-2X_{Qc}\sin\hat{\theta}_0-2X_{Qs}\cos\hat{\theta}_0.\end{aligned} \tag{32}$$

With respect to A_0 and A_1 in (31), it is to be noticed that the (normalized) noise variance $\sigma_w^2=1/(2\gamma_s)$ must be known to the receiver to calculate these relationships; in the higher SNR range, however, we can skip this term without sacrificing much of the estimator performance, as it is shown in the next section.

Finally, by inspection of (19) and (20), the estimates for the DC offset are directly established as

$$\hat{d}_I = X_I - X_c\cos\hat{\theta}_0 + X_s\sin\hat{\theta}_0 \tag{33}$$

and

$$\hat{d}_Q = X_Q - \hat{g}_R X_c\sin(\hat{\theta}_0+\hat{\varphi}_R) - \hat{g}_R X_s\cos(\hat{\theta}_0+\hat{\varphi}_R). \tag{34}$$

V. Numerical Results

For binary pilot sequences with $L=500$, a (normalized) frequency offset $v_0=0.1$, and a phase offset $\theta_0=45°$, Fig. 3 shows the evolution of the root-mean-square error (RMSE) of carrier frequency and phase estimates as a function of the SNR (phase values are given in degrees); a fairly large IQ mismatch has been chosen for this purpose: $g_R=1.2$, $\varphi_R=10°$, $d_I=d_Q=0.1$ (typical deviations from the normalized values are much lower in case of a careful chip design [13]: $|\Delta g_R|=0.05$, $|\varphi_R|=5°$, $|\Delta d_I|=|\Delta d_Q|=0.05$, or even less). For comparison reasons, the square root of the CRLBs (solid lines) are illustrated as well. As can be seen, both estimates are close the theoretical limit despite of the simplification steps introduced previously; only in the higher SNR regime, the error performance degrades somewhat.

Fig. 4 depicts the RMSE of the IQ gain and phase imbalances (phase values are again shown in degrees). If the noise power is available for the evaluation of (31), we observe a small discrepancy of the estimates – indicated by (N) in Fig. 4 – to the related CRLBs. Interestingly, when the noise variance is skipped from the evaluation of (31) – indicated by (-) in Fig. 4 – the estimation of the IQ gain deteriorates significantly with decreasing SNRs, whereas no such degradation is detected with respect to the IQ phase imbalance.

Finally, Fig. 5 visualizes the error performance of the DC offset, computed according to (33) and (34). As can be seen, the simulation results are very close to the related CRLB; a small difference emerges with d_Q at lower SNRs, when no

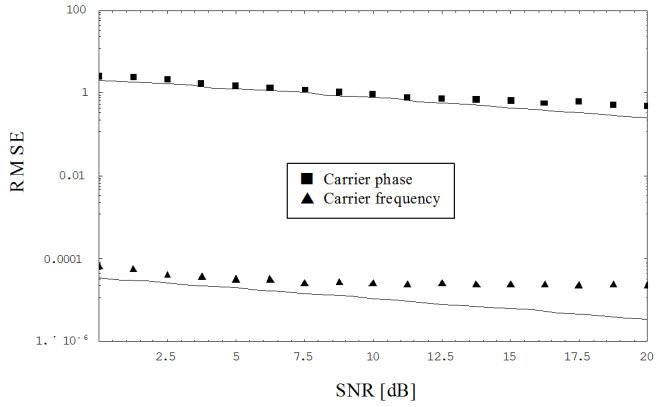

Fig. 3. Root-mean-square error of carrier frequency and phase estimates: $L = 500$, $g_R = 1.2$, $\varphi_R = 10°$, $\theta_0 = 45°$, $v_0 = 0.1$, $d_I = d_Q = 0.1$.

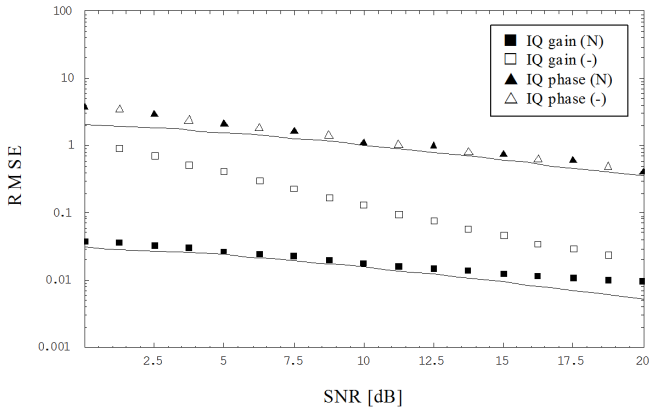

Fig. 4. Root-mean-square error of IQ gain and phase estimates: $L = 500$, $g_R = 1.2$, $\varphi_R = 10°$, $\theta_0 = 45°$, $v_0 = 0.1$, $d_I = d_Q = 0.1$.

knowledge about the noise power is assumed. Note also that the performance of d_I is a bit better than that of d_Q, which is simply explained by the fact that the noise in the Q-arm is amplified by $g_R = 1.2$.

More interesting than the RMSE evolution of the parameters to be estimated, at least from the customer point of view, is

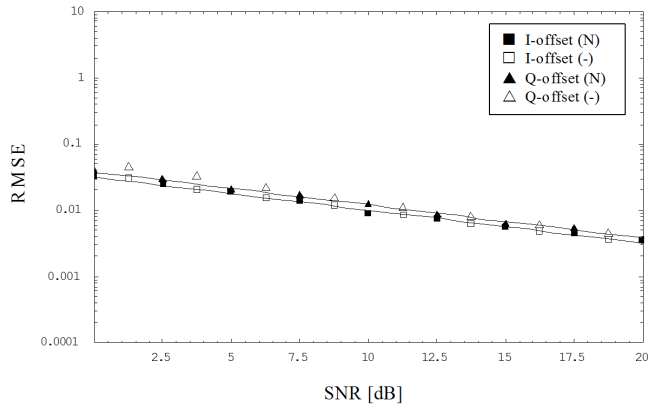

Fig. 5. Root-mean-square error of DC offset estimates: $L = 500$, $g_R = 1.2$, $\varphi_R = 10°$, $\theta_0 = 45°$, $v_0 = 0.1$, $d_I = d_Q = 0.1$.

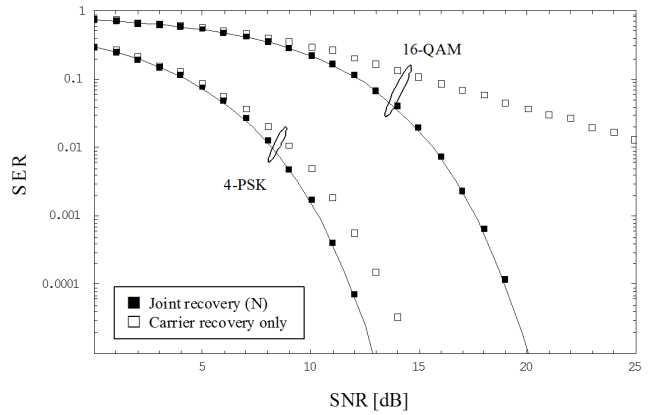

Fig. 6. Evolution of the symbol error rate (noise power assumed to be known): $L = 500$, $g_R = 1.2$, $\varphi_R = 10°$,$d_I = d_Q = 0.1$.

the symbol error rate of the received data. By choosing the same imbalance setting as before, i.e., $g_R = 1.2$, $\varphi_R = 10°$, and $d_I = d_Q = 0.1$, this has been exemplified for 4-PSK and 16-QAM constellations. In this context, we assumed a packet-oriented transmission with 1000 data symbols per block; we also assumed different frequency/phase errors per packet, randomly selected in the range $|v_0| \leq 0.1$ and $|\theta_0| \leq \pi$, respectively.

Using the linearized algorithm for parameter estimation derived in the previous section, real and imaginary parts of the data symbols c_k are detected by applying the imbalance matrix $\mathbf{\Gamma}(\cdot)$ in (10) as follows:

$$\begin{pmatrix} \hat{a}_k \\ \hat{b}_k \end{pmatrix} = \mathbf{\Gamma}^{-1}(\hat{g}_R, \hat{\varphi}_R, \hat{\theta}_0, \hat{v}_0) \begin{pmatrix} x_{k,I} - \hat{d}_I \\ x_{k,Q} - \hat{d}_Q \end{pmatrix}. \quad (35)$$

In order to cope with residual frequency errors, we suggest that each packet has a pilot sequence of 50 symbols (postamble) appended. After having accomplished the compensation process, the phase difference between preamble and postamble will be used to de-rotate the remaining carrier phase errors by linear interpolation.

Assuming that the noise power is known to the receiver, Fig. 6 shows the symbol error rate (SER) performance of the algorithm developed in Section IV (solid squares), which is – irrespective of the simplifications – very close to the theoretical curve (solid line) indicating no other distortion than zero-mean Gaussian noise. For comparison purposes, the results are presented in case that only carrier frequency/phase errors are estimated and corrected (open squares), but not the impairments introduced by IQ mismatch; in particular with respect to 16-QAM signals, a severe degradation of the SER is observed in the medium-to-high SNR range.

Ignoring the noise variance in the evaluation of (31), Fig. 7 illustrates the SER for 4-PSK and 16-QAM constellations (open squares). No performance loss is detected at lower SNR values, where the performance is mainly dominated by Gaussian noise and not so much by imperfections of the parameter estimation. It is easily verified that this holds also true for 16-QAM signals operated at higher SNRs. Using 4-PSK signals, however, one can see that the SER is seriously

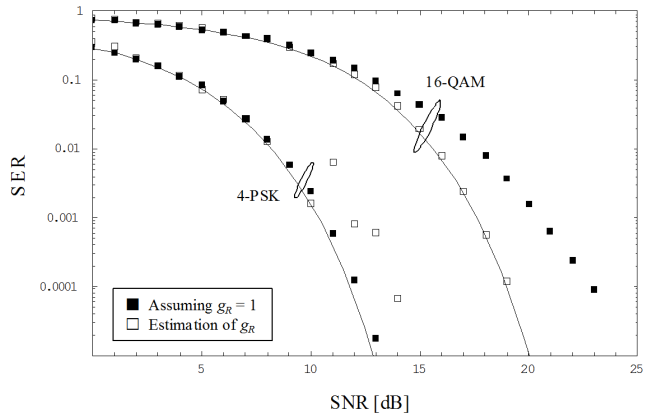

Fig. 7. Evolution of the symbol error rate (evaluation of noise power skipped): $L = 500$, $g_R = 1.2$, $\varphi_R = 10°$,$d_I = d_Q = 0.1$.

corrupted in the medium SNR domain, primarily caused by outliers of IQ gain estimates (see Fig. 4). In order to mitigate this effect, it is suggested to skip the estimation of g_R, i.e., it is assumed that g_R = 1, which results in a slightly increased SER for 4-PSK (solid squares). But with respect to 16-QAM schemes, this measure would involve a non-negligible performance loss in the medium-to-high SNR regime, as it is depicted in Fig. 7 as well.

VI. Conclusions

Motivated by the fact that the impact of carrier frequency and DC offset was neglected in some recent publications on joint recovery of carrier and imbalance parameters in direct-conversion receivers, a framework for estimating carrier frequency/phase, IQ gain/phase imbalance, and DC offset has been derived. An ML solution turned out to be available only in form of a numerical scheme, which was not pursued due to the computational load, but also because of convergence and stability problems. Instead, the focus was on the development of a closed-form algorithm by introducing several simplifications: (i) computation of the frequency offset via an estimator available from the open literature; (ii) conditioned on the frequency estimate, joint recovery of carrier phase and IQ gain/phase imbalance based on a reduced form of the likelihood function as well as neglecting the impact of the DC offset; (iii) extraction of the DC offset. Finally, it could be shown that the noise power, which forms part of the estimator framework derived in this context, need not be taken into account.

Appendix

It is assumed that we have a binary pilot sequence given by $a_k = \pm 1$ and $b_k = 0$, $k \in K = \{k_0, k_0 + 1, \ldots, k_0 + L - 1\}$. By substituting this into (10), the IQ components are obtained as $s_{k,I} = a_k \cos(2\pi k v_0 + \theta_0)$ and $s_{k,Q} = g_R a_k \sin(2\pi k v_0 + \theta_0 + \varphi_R)$. Finally, by plugging the likelihood function $\Pr(\mathbf{x}|\mathbf{u})$ into (14) and computing the corresponding derivatives, we find the FIM elements after some tedious but straightforward expectation operations:

$$F_{11} = \frac{L(1+\sec^2\varphi_R)}{g_R^2} + \frac{\sec^2\varphi_R}{g_R^2\sigma_w^2}\sum_{k\in K}\sin^2(2\pi k v_0+\theta_0+\varphi_R), \tag{36}$$

$$F_{12} = -\frac{L\sec^2\varphi_R\sin(2\varphi_R)}{2g_R} + \frac{\sec^2\varphi_R}{2g_R\sigma_w^2}\sum_{k\in K}\sin(4\pi k v_0 + 2\theta_0 + 2\varphi_R), \tag{37}$$

$$F_{13} = \frac{\sec\varphi_R}{g_R\sigma_w^2}\sum_{k\in K}\cos(2\pi k v_0+\theta_0)\sin(2\pi k v_0+\theta_0+\varphi_R), \tag{38}$$

$$F_{14} = \frac{\pi}{g_R\sigma_w^2}\sum_{k\in K}k[\sec\varphi_R\sin(4\pi k v_0 + 2\theta_0 + \varphi_R)+\tan\varphi_R], \tag{39}$$

$$F_{15} = -\frac{\sec\varphi_R\tan\varphi_R}{g_R\sigma_w^2}\sum_{k\in K}a_k\sin(2\pi k v_0+\theta_0+\varphi_R), \tag{40}$$

$$F_{16} = \frac{\sec^2\varphi_R}{g_R^2\sigma_w^2}\sum_{k\in K}a_k\sin(2\pi k v_0+\theta_0+\varphi_R), \tag{41}$$

$$F_{22} = \frac{L\sec^2\varphi_R[1+3\sigma_w^2-\sigma_w^2\cos(2\varphi_R)]}{2\sigma_w^2} + \frac{\sec^2\varphi_R}{2\sigma_w^2}\sum_{k\in K}\cos(4\pi k v_0+2\theta_0+2\varphi_R), \tag{42}$$

$$F_{23} = \frac{\sec\varphi_R}{\sigma_w^2}\sum_{k\in K}\cos(2\pi k v_0+\theta_0)\cos(2\pi k v_0+\theta_0+\varphi_R), \tag{43}$$

$$F_{24} = \frac{\pi K_1}{\sigma_w^2}+\frac{\pi\sec\varphi_R}{\sigma_w^2}\sum_{k\in K}k\cos(4\pi k v_0+2\theta_0+\varphi_R), \tag{44}$$

$$F_{25} = -\frac{\sec\varphi_R\tan\varphi_R}{\sigma_w^2}\sum_{k\in K}a_k\cos(2\pi k v_0+\theta_0+\varphi_R), \tag{45}$$

$$F_{26} = \frac{\sec^2\varphi_R}{g_R\sigma_w^2}\sum_{k\in K}a_k\cos(2\pi k v_0+\theta_0+\varphi_R), \tag{46}$$

$$F_{33} = \frac{L}{\sigma_w^2}, \tag{47}$$

$$F_{34} = \frac{2\pi}{\sigma_w^2}\sum_{k\in K}k, \tag{48}$$

$$F_{35} = -\frac{\sec\varphi_R}{\sigma_w^2}\sum_{k\in K}a_k\sin(2\pi k v_0+\theta_0+\varphi_R), \tag{49}$$

$$F_{36} = \frac{\sec\varphi_R}{g_R\sigma_w^2}\sum_{k\in K}a_k\cos(2\pi k v_0+\theta_0), \tag{50}$$

$$F_{44} = \frac{4\pi^2}{\sigma_w^2}\sum_{k\in K}k^2, \tag{51}$$

$$F_{45} = -\frac{2\pi\sec\varphi_R}{\sigma_w^2}\sum_{k\in K}ka_k\sin(2\pi k v_0+\theta_0+\varphi_R), \tag{52}$$

$$F_{46} = \frac{2\pi\sec\varphi_R}{g_R\sigma_w^2}\sum_{k\in K}ka_k\cos(2\pi k v_0+\theta_0), \tag{53}$$

$$F_{55} = \frac{L \sec^2 \varphi_R}{\sigma_w^2},\ F_{56} = -\frac{L \sec \varphi_R \tan \varphi_R}{g_R \sigma_w^2}, \tag{54}$$

$$F_{66} = \frac{L \sec^2 \varphi_R}{g_R^2 \sigma_w^2}. \tag{55}$$

Additional averaging with respect to the zero-mean pilot symbols $a_k = \pm 1$ yields the modified Cramer-Rao lower bound (MCRLB), which is less tight than the true CRLB as shown in [23] and [26], i.e., $\mathrm{Var}(u_i) \geq \mathrm{CRLB}(u_i) \geq \mathrm{MCRLB}(u_i)$. In this case, the FIM becomes block-diagonal: $F_{ij} = F_{ji} = 0$, where $i \in \{1, 2, 3, 4\}$ and $j \in \{5, 6\}$, which means that the estimation of the DC offset is decoupled from the rest of the parameter vector.

REFERENCES

[1] B. Razavi, "Design considerations for direct-conversion receivers," *IEEE Trans. Circuits Syst. II*, vol. 44, pp. 428–435, Jun. 1997.

[2] S. Mirabbasi and K. Martin, "Classical and modern receiver architectures," *IEEE Commun. Mag.*, vol. 38, pp. 132–139, Nov. 2000.

[3] W. Kogler, W. Gappmair, and O. Koudelka, "Software-radio architecture for preambleless acquisition of frame, carrier and timing in MF-TDMA modems," in *Proc. IEEE 2nd Int. Symp. Wireless Commun. Systems*, Sep. 2005, pp. 837–841.

[4] R. Bagheri, A. Mirzaei, M. E. Heidari, S. Chehrazi, M. Lee, M. Mikhemar, W. K. Tang, and A. A. Abidi, "Software-defined radio receiver: dream to reality," *IEEE Commun. Mag.*, vol. 44, pp. 111–118, Aug. 2006.

[5] X. Huang, "On transmitter gain/phase imbalance compensation at receiver," *IEEE Commun. Lett.*, vol. 4, pp. 363–365, Nov. 2000.

[6] J. K. Cavers and M. W. Liao, "Adaptive compensation for imbalance and offset losses in direct conversion transceivers," *IEEE Trans. Veh. Technol.*, vol. 42, pp. 581–588, Nov. 1993.

[7] L. Yu and W. M. Sneglove, "A novel adaptive mismatch cancellation system for quadrature IF radio receivers," *IEEE Trans. Circuits Syst. II*, vol. 46, pp. 789–801, Jun. 1999.

[8] M. Valkama, M. Renfors, and V. Koivunen, "Advanced methods for i/q imbalance compensation in communication receivers," *IEEE Trans. Signal Process.*, vol. 49, pp. 2335–2344, Oct. 2001.

[9] R. Cherukuri and P. T. Balsara, "Iterative (turbo) I/Q imbalance estimation and correction in BICM-ID for flat fading channels," in *Proc. IEEE Vehicular Technol. Conf.*, Sep. 2007, pp. 2070–2074.

[10] G. Xing, M. Shen, and H. Liu, "Frequency offset and I/Q imbalance compensation for direct-conversion receivers," *IEEE Trans. Wireless Commun.*, vol. 4, pp. 673–680, Mar. 2005.

[11] F. Horlin, A. Bourdoux, E. Lopez-Estraviz, and L. Van der Perre, "Low-complexity EM-based joint CFO and I/Q imbalance acquisition," in *Proc. IEEE Int. Commun. Conf.*, Jun. 2007, pp. 2871–2876.

[12] H. Lin, X. Zhu, and K. Yamashita, "Low-complexity pilot-aided compensation for carrier frequency offset and I/Q imbalance," *IEEE Trans. Commun.*, vol. 58, pp. 448–452, Feb. 2010.

[13] L. Giugno, V. Lottici, , and M. Luise, "Efficient compensation of I/Q phase imbalance for digital receivers," in *Proc. IEEE Int. Commun. Conf.*, May 2005, pp. 2462–2466.

[14] ——, "Low-complexity gain and phase I/Q mismatch compensation using orthogonal pilot sequences," in *Proc. European Signal Processing Conf.*, Sep. 2006, pp. 1–5.

[15] S. Park and D. Yoon, "An alternative expression for the symbol-error probability of MPSK in the presence of I/Q unbalance," *IEEE Trans. Commun.*, vol. 52, pp. 2079–2081, Dec. 2004.

[16] W. Gappmair and O. Koudelka, "CRLB and low-complex algorithm for joint estimation of carrier frequency/phase and I/Q imbalance in direct-conversion receivers," in *Proc. IEEE 8th Int. Symp. Commun. Systems, Networks and Digital Signal Processing*, Jul. 2012, pp. 1–5.

[17] I.-H. Sohn, E.-R. Jeong, and Y. H. Lee, "Data-aided approach to I/Q mismatch and DC offset compensation in communication receivers," *IEEE Commun. Lett.*, vol. 6, pp. 547–549, Dec. 2002.

[18] G.-T. Gil, I.-H. Sohn, J.-K. Park, and Y. H. Lee, "Joint ML estimation of carrier frequency, channel, I/Q mismatch, and DC offset in communication receivers," *IEEE Trans. Veh. Technol.*, vol. 54, pp. 338–349, Jan. 2005.

[19] J. G. Proakis, *Digital Communications*. McGraw-Hill: New York, 1989.

[20] A. Papoulis, *Probability, Random Variables, and Stochastic Processes*. McGraw-Hill: New York, 1991.

[21] S. M. Kay, *Fundamentals of Statistical Signal Processing: Estimation Theory*. Prentice Hall: Upper Saddle River, NJ, 1993.

[22] W. H. Press, S. A. Teukolsky, W. T. Vetterling, and B. P. Flannery, *Numerical Recipes in C: The Art of Scientific Computing*. Cambridge Univ. Press: New York, 1994.

[23] U. Mengali and A. N. D'Andrea, *Synchronization Techniques for Digital Receivers*. Plenum Press: New York, 1997.

[24] M. Morelli and U. Mengali, "Feedforward frequency estimation for PSK: a tutorial review," *Euro. Trans. Telecomms.*, vol. 9, pp. 103–116, March/April 1998.

[25] ——, "Data-aided frequency estimation for burst digital transmission," *IEEE Trans. Commun.*, vol. 45, pp. 23–25, Jan. 1997.

[26] F. Gini, R. Reggiannini, and U. Mengali, "The modified Cramer-Rao bound in vector parameter estimation," *IEEE Trans. Commun.*, vol. 46, pp. 52–60, Jan. 1998.

Wilfried Gappmair studied Communications Engineering and Computer Science at Graz University of Technology, Austria, both finished with honors in 1986 and 1991, respectively. In the sequel, he worked on his doctoral thesis and graduated in 1994 with a Ph.D. degree in Engineering Sciences. Since 1987 he participates in numerous national as well as international projects. Currently, he holds the position of an Assistant Professor at the Institute of Communication Networks and Satellite Communications. His main interests and research activities include communication theory, channel coding, digital modulation, as well as parameter estimation and synchronization in digital receivers.

Otto Koudelka is Professor for Communications Engineering and Head of the Institute of Communication Networks and Satellite Communications at Graz University of Technology, Austria. He performed research at the Rutherford-Appleton Laboratory in 1990 and was a Visiting Professor at the University of Kansas from 1999 to 2000. He is a member of the COST Telecommunications Technical Committee, several ESA working and advisory groups, former chairman of the COST-226 project, and a member of the ESA design team for the CODE experiment. His major activities include broadband wireless communications, development of satellite and terrestrial network systems, as well as the execution of tele-medicine/ science/ education and DVB-T trials.